Fourier condition links the focal length of both diffractive elements with the separation d between them. At the same time, the scale factor of the achromatic Fraunhofer diffraction pattern can be varied by simply shifting the input along the optical axis of the system. Experimental results are shown in Figures 1b and 1c.

We also demonstrated that a refractive objective and a third diffractive lens, added properly to the Figure 1a setup, transform back to the spatial domain keeping the chromatic correction. The whole arrangement then acts as an achromatic Fourier processor.[2] This broadband Fourier processor performs, with a single filter, the same spatial filtering operation for all the spectral components of the broadband source simultaneously. Of course, in addition to coherent noise suppression, this spatial-filtering configuration allows us to deal with color inputs.

From a practical point-of-view, the above setups permit, in a direct manner, the extension of some of the monochromatic information processing techniques to broadband signal processing. In particular, we mention an achromatic Vander Lugt correlator for color pattern recognition, where a conventional monochromatic complex filter matches all the monochromatic channels simultaneously. An exhaustive field of new applications is now open. The potential possibilities range from parallel color pattern recognition, sunlight optical correlation, color data security, and optical encryption systems to light-pulse shaping.

The above results can also be extended to the Fresnel diffraction region. In this case, we demonstrated that a single diffractive lens can provide an achromatic version of a selected Fresnel diffraction pattern.[3] The axial location of the input permits the sequential variation of the Fresnel diffraction pattern that is achromatized. As a first but powerful application of this result, we present a method based on the fractional Talbot effect to implement a simple array illuminator with a variable density of white-light spots comprising only a periodic refractive microlens array and a diffractive lens.[4]

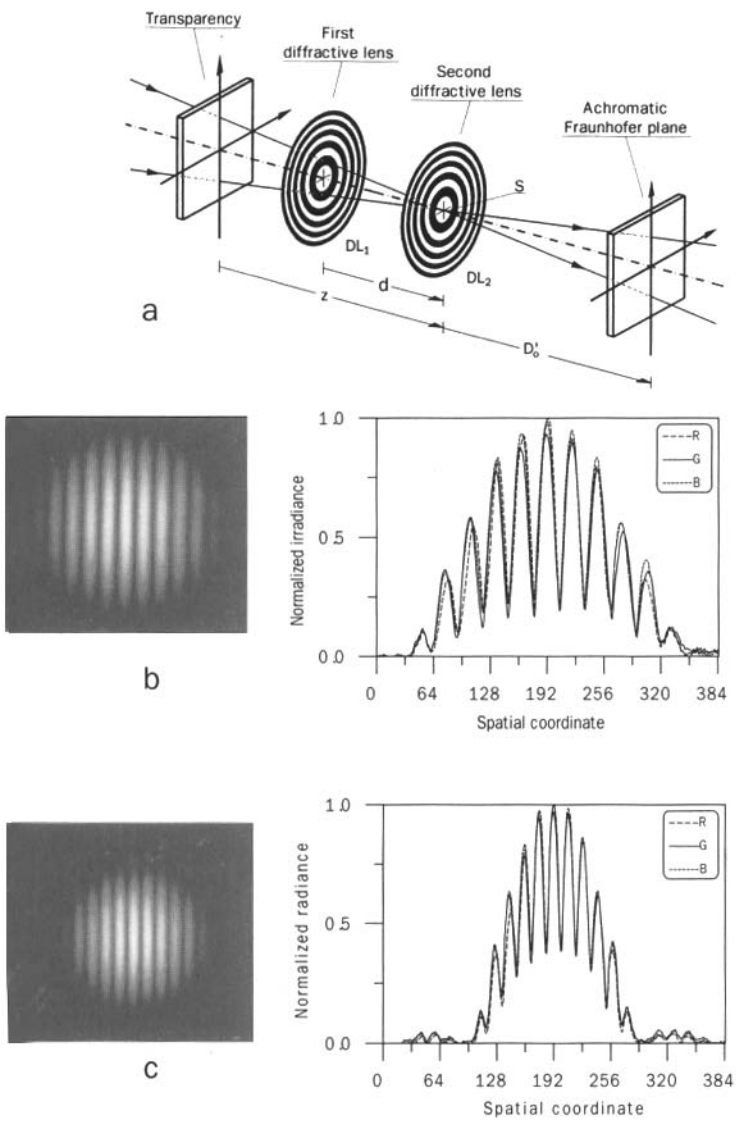

Andrés Figure 1. (a) Outline of our scale-tunable achromatic Fourier transformer. (b) and (c) Images of the irradiance distribution at the achromatic Fraunhofer plane of the above setup when the input, a double circular aperture illuminated by a high-pressure xenon arc lamp, is located in two different axial positions. The horizontal RGB-irradiance profile is also plotted. It is noteworthy that the period of the high-contrast white-light Young fringes is different in each image, while at the same time preserving the same value for all the wavelengths. (See color image, page 15.)

Acknowledgment

This work was financially supported by the Ministerio de Educacion y Ciencia (grant PB93-0354-CO2-02), Spain.

References

1. E. Tajahuerce *et al.*, "Achromatic Fourier transforming properties of a separated diffractive lens doublet: Theory and experiment," Appl. Opt. **37,** 6164–6173 (1998).
2. E. Tajahuerce *et al.*, "Hybrid (refractive-diffractive) Fourier processor: A novel optical architecture for achromatic processing with broadband point-source illumination," Opt. Commun. **151,** 86–92 (1998).
3. J. Lancis *et al.*, "Single-zone-plate achromatic Fresnel-transform setup: Pattern tunability," Opt. Commun. **136,** 297–305 (1997).
4. E. Tajahuerce *et al.*, "White-light modified Talbot array illuminator with a variable density of light spots," Appl. Opt. **37,** 4366–4373 (1998).

Artificial Dielectrics Boost Diffraction Efficiency in Diffractive Optical Elements

Philippe Lalanne, Simion Astilean, and Pierre Chavel, Laboratoire Charles Fabry de l'Institut d'Optique, Centre National de la Recherche Scientifique, Orsay, France; Edmond Cambril and Huguette Launois, Laboratoire de Microstructures et de Microélectronique, Centre National de la Recherche Scientifique, Bagneux, France.

Blazed échelette diffractive optical elements (DOEs) currently manufactured by diamond turning or direct laser-beam writing offer nearly-100% efficiency for zone widths or grating periods much larger than the wavelength. In practice, however, performance decreases[1] in the so-called resonance domain, *i.e.*, when zone widths or grating periods are equal to a few wavelengths. This is due to both theoretical limitations and fabrication problems encountered when monitoring together continuous profiles and sharp vertical edges. Ob-

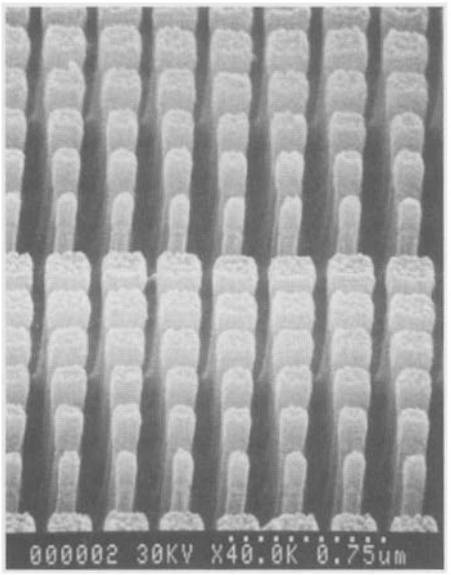

Lalanne Figure 1. SEM of a blazed-binary grating composed of subwavelength pillars etched in a TiO_2 film deposited on a glass substrate. The horizontal period (or sampling period) is equal to 272 nm and the period in the perpendicular direction is 1.9 μm. The grating depth is ≈816 nm and the maximum pillar aspect-ratio is ≈8.8.

taining high diffraction efficiency with large deflection angles is a challenge in design and fabrication of tomorrow's DOEs.

We have developed methods for the synthesis and fabrication of DOEs, called "blazed-binary" DOEs hereafter, which substantially outperform conventional blazed-échelette DOEs in the resonance domain. In our elements, each period (or zone) is composed of binary nano-pillars arranged on a square subwavelength grid and etched in a dielectric material (see Fig. 1).

By monitoring the local fraction of matter removed, we implement continuous phase delays and obtain strong blazing effects. The design exploits the analogy between subwavelength gratings and artificial dielectric materials.[2] The analogy is accurate when the distance between the subwavelength period of the square grid is smaller than some structural cut-off related to wave propagation in the nano-pillar region.[3]

Only one lithographic step is necessary for the fabrication. The process involves electron-beam lithography in a polymethyl methacrylate film, lift-off with an intermediate Nickel layer, and reactive ion etching of a TiO_2 film evaporated on a glass substrate.[4] The lift-off technique is used to enhance the selectivity and the fidelity of the pattern transfer during the etching.

Two binary-blazed DOEs with square-grid periods smaller than the structural cut-off have been designed, fabricated, and tested. The first one, a 3 λ-period (20° deflection in air) blazed-binary grating, is shown in Figure 1. For unpolarized light at 633 nm, the experimental diffraction efficiency in the transmitted first-order is 82%, a value 6% below theory. The grating behavior is nearly independent on polarization; the first-order efficiencies are 80% and 84% for TE and TM polarizations, respectively. As a matter of comparison, the maximum theoretical diffraction efficiency achieved by a transmission échelette grating in glass blazed in the first-order with a 3λ-period is 66.5%. Our second DOE is a 20° off-axis diffractive lens with a focal length of 400 μm, and a square pupil of 200 × 200 μm^2. The minimum and maximum zone widths are 1.91 λ and 8.83 λ, respectively, and half of the lens area is concerned with zone widths smaller than 2.8 λ. When measured with a vertical-cavity-surface-emitting laser emitting a Gaussian beam circularly polarized at 860 nm, a first-order diffraction efficiency of 80% is obtained. In addition to efficiency, the inspection of the point-spread function reveals a good operation.

Acknowledgment

This work was supported by the European Community under the RODCI Mel-Ari programme. The authors are grateful to Jean Landreau and Alain Carenco (Centre National des Etudes de Télécommunications; CNET-Bagneux) for coating the TiO_2 films.

References

1. T. Hessler *et al.*, "Analysis and optimization of fabrication of continuous-relief diffractive optical elements," Appl. Opt. **37,** 4069–4079 (1998).
2. W. Stork *et al.*, "Artificial distributed-index media fabricated by zero-order gratings," Opt. Lett. **16,** 1921–1923 (1991).
3. P. Lalanne *et al.*, "Blazed-binary subwavelength gratings with efficiencies larger than those of conventional échelette gratings," Opt. Lett. **23,** 1081–1083 (1998).
4. S. Astilean *et al.*, "High efficiency subwavelength element patterned in a high-refractive-index material for 633 nm," Opt. Lett. **23,** 552–554 (1998).

Gaussian Wave Packets in Resonant Diffraction Gratings

Frank Schreier, Martin Schmitz, and Olof Bryngdahl, Physics Dept., Univ. of Essen, Essen, Germany.

Resonant diffraction gratings are frequently used as convenient and flexible wavelength filters since they offer a reflectance >99% for their central wavelength, whereas far off the central wavelength the reflectance can fall below 1%. The central wavelength can be adjusted by the choice of the angle of incidence, and the FWHM of the filter can be fixed over a wide range during the design process. Resonance effects occur due to the coupling of the incident wave to guided modes supported by a waveguide layer of the structure. Numerical considerations concerning resonant gratings are usually carried out under the assumption of an incident plane wave.

We numerically investigated the spatial behavior of a Gaussian beam[1] and the temporal behavior of a Gaussian pulse[2] incident on a diffractive structure under resonance conditions. Two different geometries are considered: a waveguide grating, where the relative permittivity of a guiding layer exhibits a sinusoidal modulation (see Fig. 1a, page 22), and a waveguide structure, where the waveguide layer is separated from a substrate by a gap layer with low relative permittivity (see Fig. 1b). The coupling mechanism that results in a resonance is different for the two geometries presented. It was demonstrated that in both geometries a beam may undergo a lateral displacement, similar to the Goos-Hänchen-shift, which can grow as large as the order of the beam width; for a beam having a half-width of 9.3 mm, a lateral displacement of 5.2 mm has been observed. This displacement is several orders of magnitude larger compared to the Goos-Hänchen-shift. Additionally it is shown that only the given beam width imposes a restriction on the maximum achievable displacement.